

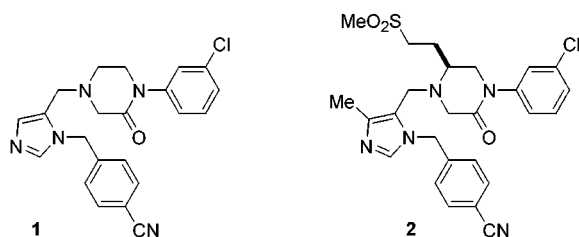
## Conformational Restriction of Flexible Ligands Guided by the Transferred NOE Experiment: Potent Macrocyclic Inhibitors of Farnesyltransferase

Christopher J. Dinsmore,<sup>\*,†</sup> Michael J. Bogusky,<sup>†</sup>  
J. Christopher Culberson,<sup>§</sup> Jeffrey M. Bergman,<sup>†</sup>  
Carl F. Homnick,<sup>†</sup> C. Blair Zartman,<sup>†</sup> Scott D. Mosser,<sup>‡</sup>  
Michael D. Schaber,<sup>‡</sup> Ronald G. Robinson,<sup>‡</sup>  
Kenneth S. Koblan,<sup>‡</sup> Hans E. Huber,<sup>‡</sup> Samuel L. Graham,<sup>†</sup>  
George D. Hartman,<sup>†</sup> Joel R. Huff,<sup>†</sup> and Theresa M. Williams<sup>†</sup>

Departments of Medicinal Chemistry  
Molecular Systems, and Cancer Research  
Merck Research Laboratories  
West Point, Pennsylvania 19486

Received October 16, 2000

The optimization of enzyme inhibitor potency and specificity is an important goal of drug design since both properties contribute to clinical efficacy and safety. Restricting an inhibitor's conformation to one recognized by the enzyme increases potency by lowering the entropic barrier to complex formation, and could potentially enhance specificity by limiting its interactions with other macromolecules.<sup>1</sup> In lieu of detailed structural characterization of enzyme–inhibitor interactions, the transferred nuclear Overhauser effect (trNOE) NMR method has proven valuable in defining conformations of ligands weakly associated with macromolecules.<sup>2</sup> However, despite the considerable implications of the trNOE technique for drug design, there are few instances of the method playing an influential role in inhibitor optimization,<sup>3</sup> and none is directed at designing specific conformational constraints. This report describes the design of a highly potent macrocyclic enzyme inhibitor based on the trNOE structure of a conformationally flexible analogue.



Farnesyltransferase (FTase) is an important posttranslational processing enzyme that prenylates proteins using farnesylpyrophosphate (FPP) and enables the participation by some in signal transduction during cell proliferation.<sup>4</sup> Inhibitors of this enzyme (FTIs) are promising antitumor agents, and several are currently being evaluated in human clinical trials.<sup>5</sup> In our investigations of

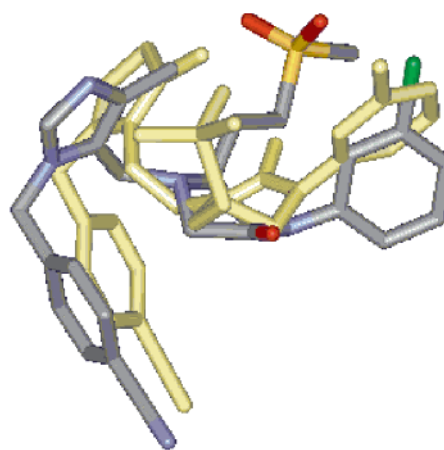


**Figure 1.** Superposition of two representative lowest-energy FTase-bound conformations of **2** consistent with trNOE-derived restraints.

structure–activity relationships of the clinical candidate **1**,<sup>6</sup> we found that the related FTI **2**, with diminished inhibitory activity (FTase IC<sub>50</sub> 475 nM vs 2 nM), was an appropriate ligand for the trNOE experiment.

In the absence of added enzyme, NMR spectroscopic evaluation of **2** reveals no defined solution conformation. NMR-derived intramolecular distance constraint data was generated in the presence of the putative FTase:FPP complex. Ligand-competition experiments with a potent peptidomimetic FTI served to disqualify non-active-site bound contributions. The calculated lowest-energy structures depict folded conformations with the cyanophenyl group flanking the piperazinone ring (Figure 1).<sup>7a</sup> Stabilization of this orientation by covalent linkage of the cyanophenyl and piperazinone *N*-aryl substituent in a macrocycle appeared to be an attractive approach to optimize the properties of **1**.

The synthesis of a macrocyclic version of **1** is described in Scheme 1. The piperazinone **8**, prepared by a Mitsunobu cyclodehydration reaction,<sup>8</sup> was reductively coupled with aldehyde **5** to give **9**. Compound **9** was subjected to a tandem base-promoted arylmethanesulfonate deprotection and S<sub>N</sub>Ar cyclization<sup>9</sup> to give the cyclophane **10** in good yield. Interestingly, **10** exhibits planar chirality, and its enantiomeric conformers are readily resolved by chiral HPLC, due to a sufficient activation energy for their interconversion.<sup>10</sup>

The calculated lowest-energy structure of (+)-**10**<sup>7c</sup> (Figure 2, gray) bears close resemblance to available FTase-bound conformations of **2** (Figure 1), especially with regard to the relative positions of the piperazinone, imidazole, and cyanophenyl rings.<sup>11</sup> Variable temperature <sup>1</sup>H NMR studies of (+)-**10** revealed

(4) (a) Kato, K.; Cox, A. D.; Hisaka, M. M.; Graham, S. M.; Buss, J. E. *Proc. Natl. Acad. Sci. U.S.A.* **1992**, *89*, 6403–6407. (b) Rowinsky, E. K.; Windle, J. L.; Von Hoff, D. D. *J. Clin. Oncol.* **1999**, *17*, 3631–3652.

(5) (a) Oliff, A. *Biochim. Biophys. Acta* **1999**, *1423*, C19–C30. (b) End, D. W. *Invest. New Drugs* **1999**, *17*, 241–258. (c) Gibbs, J. B. *J. Clin. Invest.* **2000**, *105*, 9–13.

(6) Williams, T. M.; et al., Merck & Co., Inc. unpublished data.

(7) (a) Distance restraints from trNOE data for **2** were used to generate conformations using JG (Kearsley, S. Merck & Co., Inc., unpublished). These were minimized within MacroModel (ref 7b) using the MMFF force field with a 4r distance-dependent dielectric, and with trNOE distance constraints applied. (b) Mohamadi, F.; Richards, N. G. J.; Guida, W. C.; Liskamp, R.; Caufield, C.; Chang, G.; Hendrickson, T.; Still, W. C. *J. Comput. Chem.* **1990**, *11*, 440–467. (c) Same as 7a, but without distance restraints. (d) Same as 7a, but with solution <sup>1</sup>H NMR NOE distance restraint data for (+)-**10**.

(8) Weissman, S. A.; Lewis, S.; Askin, D.; Volante, R. P.; Reider, P. J. *Tetrahedron Lett.* **1998**, *39*, 7459–7462.

(9) Dinsmore, C. J.; Zartman, C. B. *Tetrahedron Lett.* **1999**, *40*, 3989–3990.

(10) Kinetic data for the racemization of (–)-**10** in DMSO: *E*<sub>a</sub> = 28.4 kcal/mol; *t*<sub>1/2</sub> (100 °C) = 60 min; *t*<sub>1/2</sub> (120 °C) = 8.5 min; Δ*H*<sup>‡</sup> = 26.9 kcal/mol; Δ*S*<sup>‡</sup> = 12.4 eu.

<sup>†</sup> Department of Medicinal Chemistry.

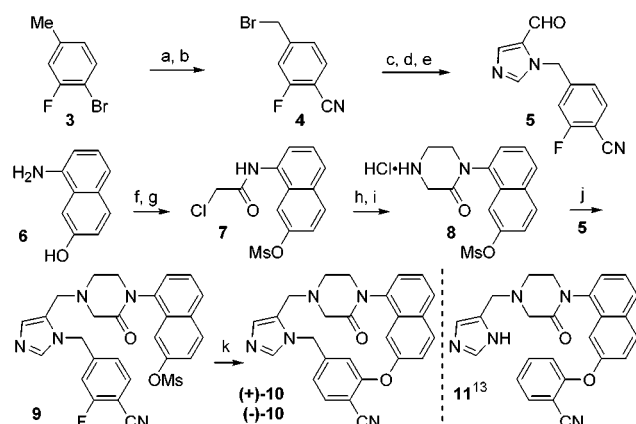
<sup>§</sup> Department of Molecular Systems.

<sup>‡</sup> Department of Cancer Research.

(1) (a) Freidinger, R. M.; Veber, D. F.; Perlow, D. S.; Brooks, J. R.; Saperstein, R. *Science* **1980**, *210*, 656–658. (b) Liskamp, R. M. J. *Recl. Trav. Chim. Pays-Bas* **1994**, *113*, 1–19.

(2) Recent reviews: (a) Roberts, G. C. K. *Curr. Opin. Biotechnol.* **1999**, *10*, 42–47. (b) Moore, J. M. *Biopolymers* **1999**, *51*, 221–243. (c) Stockman, B. J. *Prog. Nucl. Magn. Reson. Spectrosc.* **1998**, *33*, 109–151.

(3) (a) Gonnella N. C.; Bohacek, R.; Zhang, X.; Kolossvary, I.; Paris, C. G.; Melton, R.; Winter, C.; Hu, S.-I.; Ganu, V. *Proc. Natl. Acad. Sci. U.S.A.* **1995**, *92*, 462–466. (b) Williams, T. M.; Bergman, J. M.; Brashers, K.; Breslin, M. J.; Dinsmore, C. J.; Hutchinson, J. H.; MacTough, S. C.; Stump, C. S.; Wei, D. D.; Zartman, C. B.; Bogusky, M. J.; Culberson, J. C.; Buser-Doepner, C.; Davide, J.; Greenberg, I. B.; Hamilton, K. A.; Koblan, K. S.; Kohl, N. E.; Liu, D.; Lobell, R. B.; Mosser, S. D.; O'Neill, T. J.; Rands, E.; Schaber, M. D.; Wilson, F.; Senderak, E.; Motzel, S. L.; Gibbs, J. B.; Graham, S. L.; Heimbrook, D. C.; Hartman, G. D.; Oliff, A. I.; Huff, J. R. *J. Med. Chem.* **1999**, *42*, 3779–3784.

Scheme 1<sup>a</sup>

<sup>a</sup> Reagents and conditions: (a) Zn(CN)<sub>2</sub>, Pd(PPh<sub>3</sub>)<sub>4</sub>, DMF, 80 °C, 6 h, 96%. (b) NBS, AIBN, CCl<sub>4</sub>, reflux, 3 h, 43%. (c) 1-Trityl-4-(acetoxymethyl)imidazole, EtOAc, reflux, 20 h; MeOH, reflux, 30 min, 93%. (d) LiOH, 2:1 THF–H<sub>2</sub>O, 0 °C, 2 h, 83%. (e) SO<sub>3</sub>·Py, Et<sub>3</sub>N, DMSO, 45 min, 86%. (f) ClCH<sub>2</sub>COCl, aq Na<sub>2</sub>CO<sub>3</sub>, EtOAc, 0 °C, 2 h. (g) MsCl, Et<sub>3</sub>N, DMF, 0 °C, 16 h, 79% for 2 steps. (h) H<sub>2</sub>N(CH<sub>2</sub>)<sub>2</sub>OH, *i*-PrOAc, rt, 18 h. (i) DBAD, *n*-Bu<sub>3</sub>P, EtOAc, 40 °C, 10 h; HCl, EtOH, rt to 0 °C, 78%, 2 steps. (j) Na(AcO)<sub>3</sub>BH, **5**, 4 Å sieves, DCE, 0 °C to room temperature, 14 h, 91%. (k) Cs<sub>2</sub>CO<sub>3</sub>, DMSO, 0.05 M, 80 °C, 3 h, 86%.

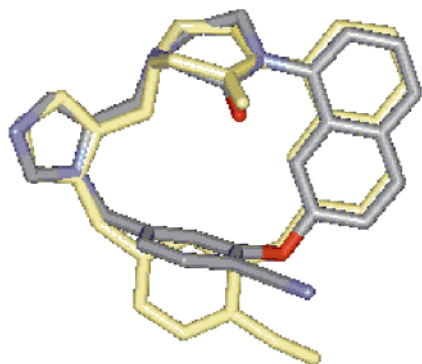


**Figure 2.** Superposition of the calculated lowest-energy conformation of (+)-**10** (gray) and the average solution structure as determined by <sup>1</sup>H NMR in *d*<sub>4</sub>-methanol (yellow).

differential line broadening below 0 °C, indicating conformational exchange, and NOE data obtained at room temperature are consistent with a mixture of available species. As such, the calculated solution structure represents an average of available conformations (Figure 2, yellow),<sup>7d</sup> largely derived from mobility of the piperazinone ring.

(11) The assignment of absolute configuration for (+)-**10** is based on X-ray crystallographic studies of the (+)-**10**·FPP·FTase complex (Beese, L. S.; Taylor, J. Duke University Medical Center, unpublished data).

(12) For assay descriptions, see refs 3b and 6. IC<sub>50</sub> (–)-**10** = 0.4 nM.

(13) Compound **11** was prepared from the naphthol corresponding to **8** by arylation (Cs<sub>2</sub>CO<sub>3</sub>, 2-fluorobenzonitrile), deprotection (HCl), and reductive alkylation with imidazole-4-carboxaldehyde (Na(AcO)<sub>3</sub>BH).

(14) The *N*-(1-naphthyl) analogue of **1** (IC<sub>50</sub> 2 nM), although equipotent to **1**, cannot bind with the same exact conformation as (+)-**10** due to overlapping hydrogen atoms. The same may be true for **11** vs (+)-**10**.

(15) Lineweaver–Burke analyses showed that (+)-**10** and **1** are competitive with K-Ras protein, and not competitive with FPP. The mechanism of binding for **11** is unknown and is assumed to be the same as for **1** and (+)-**10**, based on similar structure.

(16) For a good discussion of this analysis, see: Khan, A. R.; Parrish, J. C.; Fraser, M. E.; Smith, W. W.; Bartlett, P. A.; James, M. N. G. *Biochemistry* **1998**, *37*, 16839–16845 and references therein.

(17) Go, N.; Scheraga, H. A. *Macromolecules* **1970**, *3*, 178–187.

(18) Cheng, Y.-C.; Prusoff, W. H. *Biochem. Pharmacol.* **1973**, *22*, 3099.

**Table 1.** FTase Inhibition Data and Effect of Constraining Bond Rotations

compd	IC <sub>50</sub> (nM) <sup>a</sup>	K <sub>i</sub> (nM) <sup>b</sup>	effect of constraint on binding energy (kcal/mol) <sup>c</sup>		number available bond rotations <sup>d</sup>
			ΔΔG <sup>o</sup>	per bond	
(+)- <b>10</b>	0.1	0.20 ± 0.06	–	–	9–6 = 3 <sup>e</sup>
<b>1</b>	2	0.9 ± 0.3	0.9 (1.8)	0.2 (0.4)	7
<b>11</b>	5490	nd	(6.6)	(1.6)	7

<sup>a</sup> Concentration of compound required to reduce the FTase-catalyzed incorporation of [<sup>3</sup>H]FPP into recombinant Ras-CVIM by 50%. <sup>b</sup> K<sub>i</sub> vs K-4B-Ras. <sup>c</sup> Overall free energy difference from the equation ΔΔG<sup>o</sup> = –RT[ln(K<sub>i,cyclic</sub>/K<sub>i,acyclic</sub>)] (ref 16). Values in parentheses are from estimated K<sub>i</sub>'s vs Ras CVIM (K<sub>M</sub> 18 nM), which are derived from the IC<sub>50</sub> values using the Cheng–Prusoff equation (ref 18). <sup>d</sup> Independently rotatable dihedral angles, excluding bonds in aromatic rings, amides, and C–C≡N. The three N–CH<sub>2</sub>–CH<sub>2</sub>–N bonds are also excluded, since these variables are dependent on the N–CH<sub>2</sub>–CO–N dihedrals. <sup>e</sup> Six degrees of freedom are lost on macrocyclization (ref 17).

The FTase inhibitory activity for macrocycle (+)-**10** was assessed relative to open-chain analogues (Table 1).<sup>12</sup> In principle, compounds **1** and **11**<sup>13</sup> may adopt conformations similar to (+)-**10** without suffering significant intramolecular destabilizing interactions.<sup>14</sup> Because of close structural similarities among all three compounds, differences in their enthalpic contributions to binding should be small, assuming similar binding modes.<sup>15</sup> The enhanced relative activity for (+)-**10**, therefore, suggests that the entropic disadvantage of complex formation is significantly reduced by incorporation of the macrocyclic constraint. However, the extent of this entropic penalty (estimated as ΔΔG<sup>o</sup>)<sup>16</sup> is dependent on the position of ring cleavage, even though the number of available bond rotations in **1** and **11** is the same.<sup>17</sup> The penalty for binding of **1** on a per-bond basis<sup>16</sup> relative to (+)-**10** may be an underestimate, since it is possible that the chlorine atom of **1** contributes to binding by occupying a position which is unavailable to the corresponding naphthalene CH group in (+)-**10**. Furthermore, the greater penalty for **11** may be an overestimate because of a possible increase in the enthalpy of binding due to an inability of the imidazole and cyanophenyl rings to occupy the optimal relative positions<sup>14</sup> or due to diminished binding of an N–H versus N-alkyl imidazole. Alternatively, **11** may exhibit a different binding mode relative to (+)-**10**.<sup>15</sup>

The macrocyclic conformational constraint imparts a striking change in the mechanism of inhibition of the FTase-related enzyme geranylgeranyltransferase-I (GGTase-I). Despite very similar structural elements, **1** is competitive with the geranylgeranylpyrophosphate substrate (IC<sub>50</sub> 98 nM),<sup>6</sup> while (+)-**10** is competitive with the K-Ras-derived peptide substrate used in the assay (IC<sub>50</sub> 300 nM).<sup>12</sup> This difference in mechanism suggests disparate binding modes in the GGTase-I active site for acyclic **1** and macrocyclic (+)-**10**.

In summary, the trNOE structure of a conformationally flexible member of a well-developed inhibitor structural series was used to design a macrocyclic analogue which exhibited both enhanced FTase and altered GGTase-I inhibition properties. This suggests that trNOE technology can contribute significantly to inhibitor optimization well into late stages of design.

**Supporting Information Available:** trNOE data for **2**, overlay of **2** and (+)-**10**, procedures and characterization data for compounds **3–10**, and data for the interconversion of (+)-**10** and (–)-**10** (PDF). This material is available free of charge via the Internet at <http://pubs.acs.org>.

JA003673Q